Chemical fuel-driven dissipative living materials

Hyuna Jo, [1, 2] Serxho Selmani, [1, 2] Zhibin Guan, [1, 2, 3, 4, 5] and Seunghyun Sim[1, 2, 3, 5] *

[1] Center for Complex and Active Materials, University of California, Irvine, Irvine, California 92697, United States

[2] Department of Chemistry, University of California Irvine, Irvine, California 92697, United States

[3] Department of Chemical and Biomolecular Engineering, University of California Irvine, Irvine, California 92697, United States

[4] Department of Material Science and Engineering, University of California Irvine, Irvine, California 92697, United States

[5] Department of Biomedical Engineering, University of California Irvine, Irvine, California 92697, United States

ABSTRACT: Dissipative behaviors in biology are fuel-driven processes controlled by living cells and shape the structural and functional complexities in biological materials. It has inspired the development of various forms of synthetic dissipative materials controlled by time-dependent consumption of chemical or physical fuels, such as reactive chemical species, light, and electricity. To this date, synthetic living material featuring dissipative behaviors directly controlled by the fuel consumption of their constituent cells is unprecedented. In this paper, we report a chemical fuel-driven dissipative behavior of living materials comprising *S. epidermidis* and telechelic block copolymers. The macroscopic phase transition is controlled by D-glucose which serves a dual role of a competitive disassembling agent and a biological fuel source for living cells. Our work is a significant step towards constructing a synthetic dissipative living system and provides a new tool and knowledge to design emergent living materials.

Introduction

Dissipative behaviors sculpt the structural and functional complexities of living biological materials.[1, 2] The out-of-equilibrium nature of these biological processes accompanies a flow of energy and consumption of fuel sources by living cells. For example, bone tissues – a composite living material of cells and macromolecular scaffold – undergo continuous remodeling to repair damages, adjust for changing mechanical needs, and maintain calcium homeostasis.[3-5] In this and many other examples in biological materials, the cellular metabolism of fuels (e.g., glucose) is the fundamental driving force controlling their macroscopic behaviors.

Efforts in the past decade to mimic such out-of-equilibrium control in constructing molecular assemblies have yielded various forms of synthetic dissipative materials. Pioneering works in this area have demonstrated molecular assemblies driven by chemical reaction networks where added fuel converts a precursor into an assembling or disassembling species, and a spontaneous chemical process (e.g., hydrolysis) reverts it to the precursor state.[6-9] In these systems, chemical energy in the fuel temporarily produces a transient metastable species while the fuel is converted into waste.[10-12] Other forms of energy to generate metastable states, including light,[13-15] and more recently, electricity,[16] have been introduced to construct and control dissipative materials.

An important challenge in this field is to integrate such dissipative behaviors in synthetic materials with living cells to create synthetic living materials equipped with time-dependent behaviors useful for shaping their structure and function, just like what is seen in bones. An effort to indirectly connect the dissipative behavior of synthetic materials with cellular metabolism was made by Miravet and coworkers.[17] They showed that CO_2 produced by the metabolism of sucrose by yeast cells changes the pH of the solution, inducing subsequent assembly of hydrogelators. However, synthetic living material featuring time-dependent dissipative behavior directly controlled by the cellular metabolism of fuel is unprecedented.

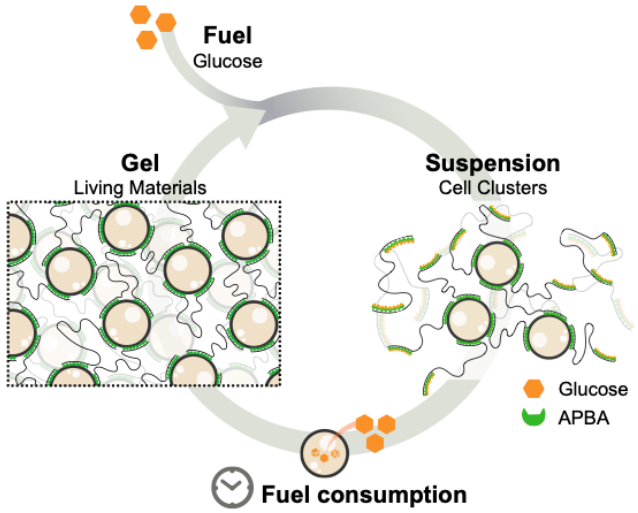

Figure 1. Design concept of fuel-driven dissipative living materials. A living material (gel) comprising *S. epidermidis* and a telechelic block copolymer bearing 3-acetamidophenylboronic acid (APBA) end block disassemble into cell clusters (suspension) following the addition of D-glucose (fuel). Time-dependent metabolic fuel consumption by living cells drives the reassembly of living materials.

Here, we report a chemical fuel-driven dissipative living material comprising bacterial cells and a telechelic block polymer containing 3-acetamidophenylboronic acid (APBA) end blocks (Figure 1). In a

previous study, we reported a series of living materials enabled by dynamic covalent bond formation between the diols on the surface teichoic acids of *Bacillus subtilis* and phenylboronic acid moiety on synthetic block copolymers.[18] These living materials disassemble upon addition of competing diols such as fructose. Given that sugars can be consumed as a fuel source for living cells, we sought to capitalize on the dual role of D-glucose, as a competitive disassembling agent and a biological fuel source for cells, to create the first dissipative living material system.

RESULTS AND DISCUSSION

The interplay between competitive binding to polymers and metabolic consumption of fuels leads to dissipative behaviors in cellular aggregates.

The bacterium in our previous study, *B. subtilis*, undergoes sporulation in nutrient-deprived conditions. Because this process hinders continuous metabolic consumption of fuels and releases cellular debris as byproducts, we chose a non-sporulating gram-positive bacterium, *Staphylococcus epidermidis*, for this study. Its thick peptidoglycan wall is decorated with teichoic acids and enables survival under various osmotic pressure.[19] We first set out to examine whether the APBA motif can target the available surface diols on *S. epidermidis*. Fluorescent probes appended with a sulfo-Cy5 (sCy5) dye (Figure 2a, 7.5 μM in PBS, pH 7.2) were incubated with suspensions of *S. epidermidis* for 3 hours at room temperature, washed with PBS twice, and subjected to fluorescence microscopy (λ_{ex} = 630 nm, λ_{obs} = 690–740 nm).[18] Fluorescence signals from the monomeric APBA probe, APBA-sCy5, were localized on the cell surface, and individual cells were mostly dispersed (Figure 2b). In contrast, fluorescent cellular aggregates were observed with the polymeric probe, poly(APBA)-sCy5, suggesting that these polymers can provide binding sites for more than one cell. Corresponding to these observations, bulk fluorescence emission (λ_{ex} = 630 nm, λ_{obs} = 650–800 nm) of these samples revealed that APBA-containing probes showed much stronger fluorescence than the cell suspension treated with Tris-sCy5 probe that bears trisaminomethane group instead of APBA motif (Figure 2d). These results support that the APBA motif binds to the *S. epidermidis* cell surface, similar to *B. subtilis*.[18]

Next, we proceeded with our design of dissipative living materials by assuming that metabolizable diols, such as fructose and glucose, can serve dual roles in this system: (1) competitive detaching agent to separate cells from polymers and (2) carbon source spontaneously metabolized by living cells over time. Three sugars were used in this study: D-glucose, L-glucose, and D-fructose. All of these sugars are known to bind to the APBA motif with different association coefficients,[20] 8.1 M^{-1} for glucose and 350 M^{-1} for fructose. We tested the dynamic behavior of bound APBA probes in the presence of these sugars by adding them (500 mM) to suspensions of labeled cells with poly(APBA)-sCy5 in PBS. At each time point, cells were washed to remove any unbound fluorescent species, and the remaining fluorescence emission from bound polymers was measured. Just after 1-hour incubation, we observed approximately an 80% decrease in fluorescence intensity in samples incubated with D- and L-glucose and near complete diminishment of fluorescent signals with D-fructose (Figure 2e). This agrees with the fact that fructose binding to APBA is two orders of magnitude stronger than glucose.[20] Microscopic observation of cells at this time point shows that large fluorescent cellular aggregates dispersed into individual cells with diminished fluorescence on their surface for all of the sugars (Figure S4). With prolonged incubation time, the fluorescence from bound

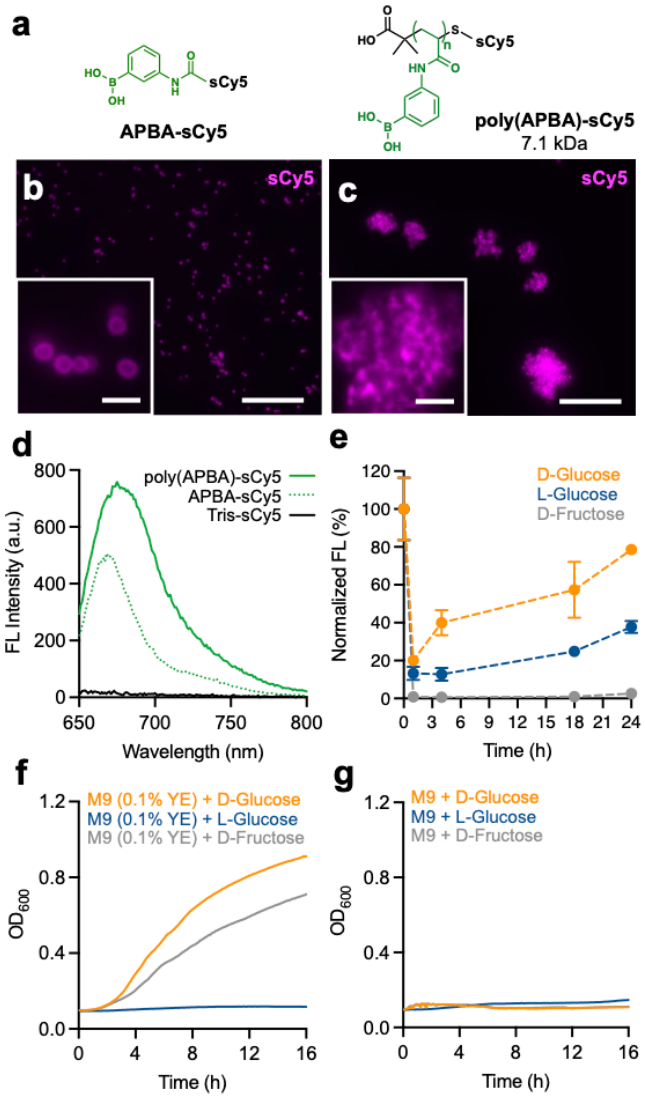

Figure 2. The interplay between competitive binding to polymers and metabolic consumption of fuels leads to dissipative behaviors in cellular aggregates. (a) Molecular structure of monomeric and polymeric APBA probes bearing a sulfo-Cy5 dye. (b–c) A representative fluorescence microscope images (λ_{ex} = 630 nm, λ_{obs} = 690–740 nm) of *S. epidermidis* cells incubated with (b) APBA-sCy5 and (c) poly(APBA)-sCy5. Scale bars = 30 μm (3 μm for inset). (d) Bulk fluorescence emission spectra (λ_{ex} = 630 nm) of *S. epidermidis* cells after 3-hours incubation with APBA-sCy5 (green, solid line), polyAPBA-sCy5 (green, dotted line), and Tris-sCy5 (black). (e) Normalized fluorescence profiles of *S. epidermidis* cell suspension first incubated with poly(APBA)-sCy5 and subsequently treated with D-glucose (orange), L-glucose (blue), and D-fructose (gray) over 24 hours. N = 3 (biological replicates). Error bars represent ± s.e.m. (f–g) Cell density probed by absorbance at 600 nm (OD_{600}) of M9 media containing D-glucose (orange), L-glucose (blue), and D-fructose (gray) in the presence (f) and the absence (g) of 0.1% yeast extract.

polymers increases in the samples containing D-glucose (Figure 2e, orange), suggesting that consumption of this sugar by cellular metabolism frees APBA binding sites from polymers and leads to reattachment to the cell surface. We also observed an increment of fluorescence in the samples incubated with L-glucose after 18 hours

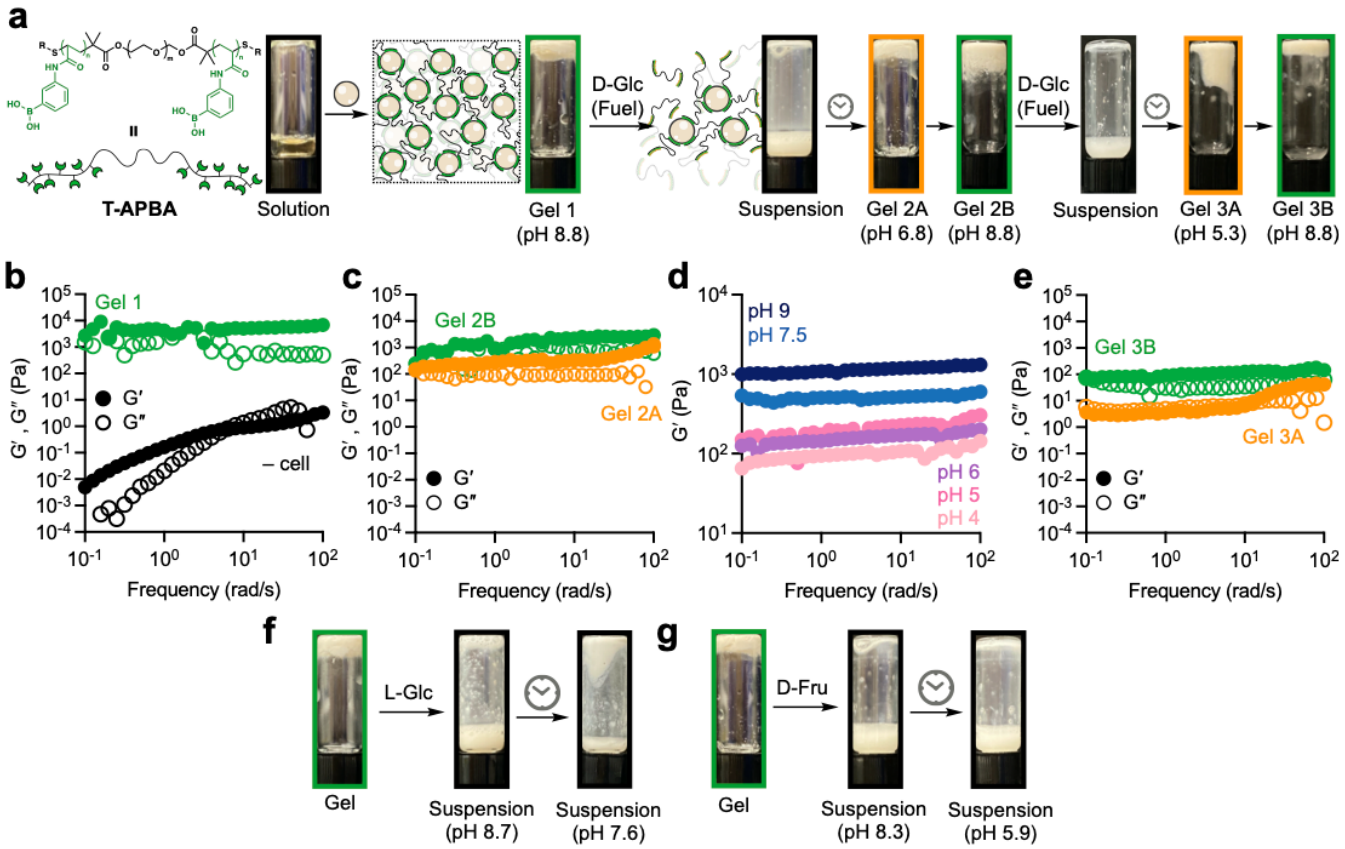

Figure 3. Glucose-driven dissipative behavior of living materials. (a) Schematic illustration and optical images of living materials showing dissipative behaviors. Gel 1, comprising T-APBA and *S. epidermidis*, disassembles into cell suspension by exogenously supplied D-glucose (fuel) and turns back into Gel 2A. After adjusting the pH, Gel 2B is subjected to another cycle, yielding a cell suspension, followed by Gel 3A and 3B. (b) Storage moduli G′ and loss moduli G″ of T-APBA in the absence (black) and the presence (green) of *S. epidermidis*. (c) Rheological characterization of Gel 2A and Gel 2B. (d) G′ values of living materials incubated at pH 4–9 for 18 hours at 30 °C. (e) Rheological characterization of Gel 3A and Gel 3B. (f–g) Optical images of living materials after immersing them into an (f) L-glucose or (g) D-fructose solution.

(Figure 2e, navy blue). In contrast, diminished fluorescence in the samples incubated with D-fructose did not recover (Figure 2e, gray). Corresponding to the bulk fluorescence measurements, fluorescent cellular aggregates were observed in cells incubated with D- and L-glucose for 24 hours (Figures S4)

To investigate whether *S. epidermidis* cells metabolize these sugars, we first prepared an M9 media supplemented with 0.1% yeast extract containing nitrogen and other necessary elements for cell division. Because cells in this media do not divide without providing extra carbon sources (Figure S6), it allows us to test whether *S. epidermidis* can metabolize these sugars by monitoring the cell density (OD_{600}) over time. In the presence of D-glucose and D-fructose (500 mM, 30 °C), *S. epidermidis* cells actively divide in the course of 16 hours (Figure 2f). However, this is not the case in the medium supplemented with L-glucose. This result demonstrates that *S. epidermidis* utilize D-glucose and D-fructose as carbon sources, but not L-glucose. It also supports our conclusion that cellular consumption of D-glucose over time leads to the reattachment of polymers to the cell surface (Figure 2e, orange). Despite that D-fructose is consumed by *S. epidermidis*, detached polymers did not reattach to the cell surface even after 24 hours (Figure 2e, gray). We suspect that because fructose binds too strongly to the polymers, they are less available for cells to consume. The small, yet noticeable increase in fluorescence in samples treated with L-glucose (Figure 2e, navy blue) might be due to the decreased pH due to the respiratory activity of the cells. Experiments performed in M9 media without 0.1% yeast extract show that cell division does not occur even when carbon sources are present (Figure 2e). All of the living materials described below are prepared without yeast extract to suppress cell division.

Fuel-driven dissipative behavior of living material.

Encouraged by the results shown above, we synthesized a telechelic polymer, T-APBA (Figure 3a; 16,740 g/mol, PEG 10,000 g/mol as mid-block, 44 units of APBA as end-block),[18] to construct macroscopic living materials showing dissipative behavior. A PBS suspension of *S. epidermidis* cells (10^{11} cells/mL in PBS, pH 7.2) was added to a solution of T-APBA (10 wt% in 80 mM PBS, pH 9.5) to afford a living material in hydrogel form (Gel 1) (Figure 3a). Linear rheological measurement showed that adding cells to a polymer solution (Figure 3b, black) makes it a viscoelastic solid (Figure 3b, green). Immersing and agitating Gel 1 in a D-glucose solution (500 mM in M9, pH 8.1, 200 rpm) at 30 °C for 3 hours converts the macroscopic network into a suspension of cell clusters (Figures 3a and S7). Further incubation and agitation of this suspension at 30 °C for 14 more hours resulted in a reformation of macroscopic gel (Gel 2A, Figure 3a), a viscoelastic solid with shear storage moduli (G′) an order of magnitude lower than the pristine Gel 1 (Figure 3c, orange). Notably, the pH of this Gel 2A (pH 6.8) was significantly lower than the pristine Gel 1 (pH 8.8) and the glucose solution (pH 8.1),

presumably due to the active cellular metabolism and consumption of carbon sources producing organic acids, such as pyruvic acid or acetic acid.[21]

We suspected that the lower G′ in Gel 2A was due to the lowered pH (pH 6.8) because the diol binding of phenylboronic acid species is known to be affected by pH.[20, 22, 23] To establish the pH-dependent changes in G′, we prepared Gel 1 samples and immersed them in PBS buffers with a pH ranging from 4 to 9. As the pH increases, G′ of Gel 1 also increases (Figure 3d). Based on this result, we adjusted the pH of Gel 2A from 6.8 to 8.8 (Gel 2B), after which G′ of Gel 2B increased by an order of magnitude (Figure 3c, green). Immersing Gel 2B to the glucose solution (500 mM in M9, pH 8.1, 200 rpm) for the second time yielded a suspension (Figure S7), and further incubation of this suspension regenerates the macroscopic network, Gel 3A (Figure 3e, orange). We note that if the pH of Gel 2A is not adjusted before subjecting them to the second cycle, it fails to generate Gel 3A. Similar to Gel 2A, Gel 3A was more acidic (pH 5.3) and exhibited lower G′ compared to Gel 2B due to the metabolic production of acidic species. Even after adjusting its pH to 8.8 (Gel 3B), G′ of the gel was significantly lower than the pristine (Gel 1) or reformed gels after the first cycle (Gel 2A and 2B) (Figure 3e, green). Using a 5-cyano-2,3-ditoyl tetrazolium chloride (CTC) reagent, we investigated the metabolic activity of the retrieved cells from these gels. By the end of the second cycle, cellular metabolic activity is decreased by 50% (Figure S11). We suspect that the reduced metabolic consumption of glucose and released cellular debris (e.g., nucleic acids) from dead cells weakened the mechanical stiffness of Gel 3A and 3B.

When Gel 1 is subjected to a solution of L-glucose (500 mM in M9, pH 8.1), the suspension does not form a gel even after 17 hours (Figures 3f and S8). The complex viscosity of the L-glucose suspension increased by 8.3-fold during this time (Figure S8), and the pH of this suspension decreased from 8.7 to 7.6. We speculate that cellular respiration lowered the pH of the suspension and changed the relative binding affinity of added L-glucose and the APBA motif. When Gel 1 is immersed in a D-fructose solution (500 mM in M9, pH 8.1), the suspension also did not revert to gel form (Figure 3g), and the complex viscosity of the suspension after 17 hours of incubation did not increase from that of 3 hours (Figure S9). The pH of this suspension also decreased from 8.3 to 5.9 presumably due to the cellular respiration and partial consumption of D-fructose. These trends are similar to the fluorescence data obtained with cellular aggregates formed by added poly(APBA) (Figure 2e).

Effect of polymer structures on dissipative behavior.

We then investigated whether polymer structures affect the dissipative behavior of the resulting living materials. Statistical copolymer with APBA motifs distributed along the polymer chain (S-APBA; Figure 4a) was synthesized via reversible addition-fragmentation chain transfer (RAFT) polymerization and subsequent end-group modification (Figures S1 and S2). S-APBA (17,413 g/mol) has a similar molecular weight to T-APBA (16,740 g/mol), according to gel permeation chromatography (Figure S3), and contains a similar number of APBA units per polymer chain (40 for S-APBA and 44 for T-APBA), based on ^{1}H NMR (Figures S1 and S2). We prepared a self-standing hydrogel by adding a cell suspension (10^{11} cells/mL) to a solution of S-APBA (20 wt% in methanol) (Figure 4b). Similar to the case of T-APBA, adding cells to the polymer solution increased the G′ by orders of magnitude (Figure 4c). These living materials were converted into suspension by immersing and

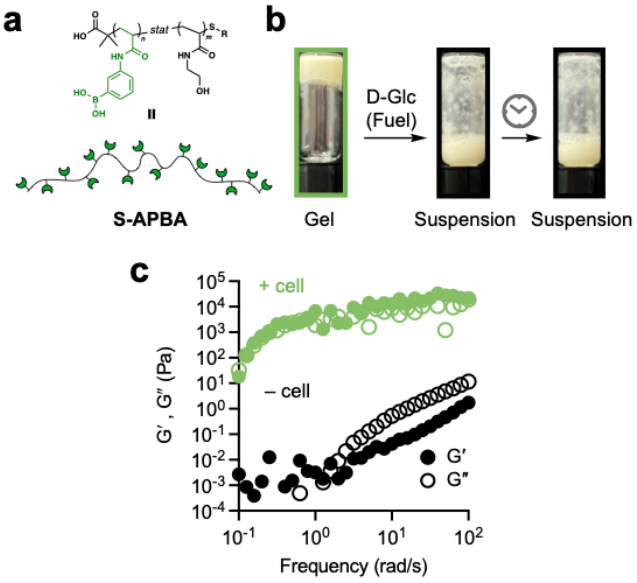

Figure 4. Effect of polymer structures on dissipative behavior. (a) Molecular structure of a statistical copolymer S-APBA bearing *N*-hydroxyethyl acrylamide and APBA. (b) Optical images of living materials comprising S-APBA and *S. epidermidis* after immersing them to a D-glucose solution. (c) Storage moduli G′ and loss moduli G″ of S-APBA in the absence (black) and the presence (green) of *S. epidermidis*.

agitating them in a D-glucose solution (500 mM in M9, pH 8.1), and strikingly, it did not reform the macroscopic network even after 17 hours of incubation (Figures 4b and S10). That S-APBA is incapable of generating dissipative behavior in living materials implies the potential multivalent effect of APBA end blocks of telechelic polymers in cellular binding.

Time-dependent fuel consumption by living cells.

Finally, we investigated D-glucose consumption by living materials at a molecular level. We quantified the extracellular concentration of glucose of living materials under dissipative cycles using colorimetric assays (Figure S12). The concentration of D-glucose was reduced by 92% in 17 hours in the course of the first cycle (Figure 5a). In contrast, the amount of D-glucose was decreased by only 58% during the second cycle, which corresponds to the weak mechanical properties of Gel 3A and 3B (Figure 2e) and reduced metabolic activity of encased cells (Figure S11). We employed a fluorescently labeled D-glucose probe to further investigate whether glucose was transported intracellularly to be consumed.[24] The cells treated with this probe were retrieved from the living materials for bulk fluorescence measurements (Figure 5b) and fluorescence microscopy (Figures 5c and S5). Both results show more intracellularly localized fluorescent probes as time goes by. Taken together, the dissipative behavior of living materials is directly driven by the time-dependent consumption of supplied glucose via cellular metabolism.

Because cells are the crosslinking points of these living materials, their mobility should correlate with the macroscopic behavior of materials and give us molecular insights into the fuel consumption process. We observed fluorescently labeled cells within living materials and cell clusters to examine cellular mobility using confocal laser scanning microscopy. About 1% of the cells within the living materials were covalently labeled with NHS-sCy5 to allow for individual cell tracking to compute each sample's mean square displacement

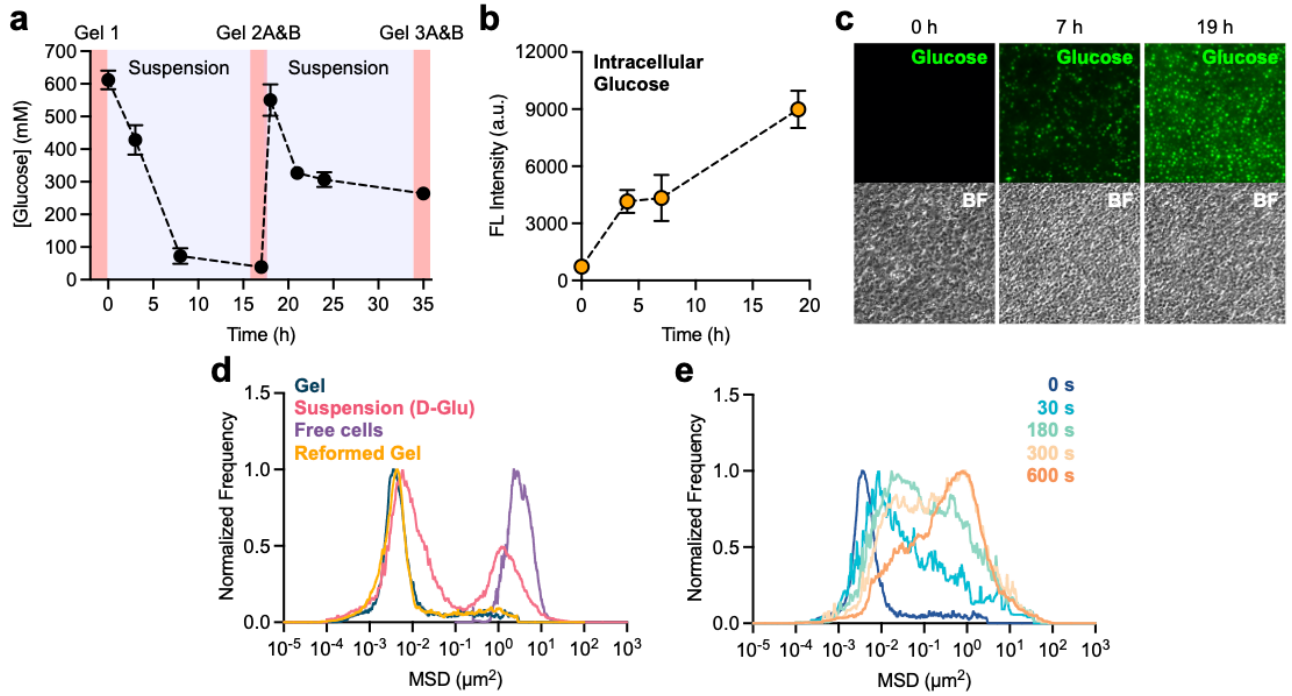

Figure 5. Time-dependent fuel consumption and cell mobility. (a) Extracellular concentration of supplied D-glucose over time. (b) Fluorescence emission of bulk suspensions of the cells retrieved from living materials (λ_{ex} = 480 nm, λ_{obs} = 520 nm) and (c) fluorescence microscope images (λ_{ex} =480 nm, λ_{obs} =520 nm) of the retrieved cells from living materials. These materials were incubated with a solution containing the fluorescently-labeled glucose probe. (d) Mean square displacement (MSD) profile of cells in pristine gel, cell suspension prepared with D-glucose, free-floating cells, and cells in reformed gel. (e) Mean square displacement (MSD) profiles of cells after *in-situ* addition of D-glucose to a pristine gel.

(MSD) profile for the cell movement (Supplementary Videos 1–4).[25] As shown in Figure 5d, gels, suspension, and free-floating cell samples showed distinct MSD profiles. Cells embedded in the living materials showed much slower movement compared to free-floating cells by a factor of ~10^3. Suspension prepared by soaking living materials in D-glucose solution shows two distinct populations, one close to free-floating cells and the other resembling cells embedded in the gel, indicating the coexistence of single cells and cell clusters. Notably, reformed gels showed a similar MSD profile to pristine gels. We then monitored the *in-situ* dissociation of living materials upon addition of D-glucose to the sample. Dissociation of cells from the edge of the gel was monitored by CLSM microscopy over time (Figure 5e and Supplementary Video 5). The population shifted to mostly free-floating cells in the course of 600 s in response to the added D-glucose.

Conclusions and Outlook.

This work reports the first dissipative living material controlled by metabolization of D-glucose by living cells. Because these materials are constructed with the dynamic covalent interface between living cells and telechelic block copolymers, D-glucose can serve as both a disassembling agent and metabolic fuel for the living materials. As a result, the macroscopic phase transition was directly controlled by the fuel consumption of living cells over time. We also investigated the effect of polymer architecture, sugar structure, and kinetics of fuel consumption at a molecular level. To the best of our knowledge, this work represents the first example of a synthetic dissipative system that directly interfaces and is controlled by living cells. It significantly expands the scope of dissipative materials by bringing it one step closer to biology. Considering that biology harnesses time-dependent restructuring mechanisms to shape many functions, this and further work may open new possibilities for creating complex living materials with emergent functions.

ASSOCIATED CONTENT

Supporting Information

The Supporting Information is available free of charge on the ACS Publications website.

AUTHOR INFORMATION

Corresponding Author

* **Seunghyun Sim** – Center for Complex and Active Materials, University of California, Irvine, Irvine, California 92697; Department of Chemistry, Department of Biomedical Engineering, Department of Chemical and Biomolecular Engineering, University of California, Irvine, California 92697, United States;
Email: s.sim@uci.edu

Author Contributions

The manuscript was written through contributions of all authors, and all authors have given approval to the final version of the manuscript.

ACKNOWLEDGMENT

This work is supported by the National Science Foundation Materials Research Science and Engineering Center program through the UC Irvine Center for Complex and Active Materials (DMR-2011967). The authors acknowledge the use of facilities and instrumentation at the UC Irvine Materials Research Institute (IMRI) supported in part by the National Science Foundation Materials Research Science and Engineering Center program through the UC Irvine Center for Complex and Active Materials (DMR-2011967). S.S. acknowledges support from an NSERC postdoctoral fellowship from the Research Council of Canada. Nuclear Magnetic Resonance measurements were done in the NMR facility in the Department of Chemistry, University of California, Irvine.

REFERENCES

(1) Karsenti, E. Self-organization in cell biology: a brief history. *Nature reviews Molecular cell biology* **2008**, *9* (3), 255-262.
(2) Lenne, P.-F.; Trivedi, V. Sculpting tissues by phase transitions. *Nature Communications* **2022**, *13* (1), 1-14.
(3) Lee, W.-C.; Guntur, A. R.; Long, F.; Rosen, C. J. Energy metabolism of the osteoblast: implications for osteoporosis. *Endocrine reviews* **2017**, *38* (3), 255-266.
(4) Hadjidakis, D. J.; Androulakis, I. I. Bone remodeling. *Annals of the New York academy of sciences* **2006**, *1092* (1), 385-396.
(5) Raggatt, L. J.; Partridge, N. C. Cellular and molecular mechanisms of bone remodeling. *Journal of biological chemistry* **2010**, *285* (33), 25103-25108.
(6) Boekhoven, J.; Brizard, A. M.; Kowlgi, K. N.; Koper, G. J.; Eelkema, R.; van Esch, J. H. Dissipative self-assembly of a molecular gelator by using a chemical fuel. *Angewandte Chemie* **2010**, *122* (28), 4935-4938.
(7) Boekhoven, J.; Hendriksen, W. E.; Koper, G. J.; Eelkema, R.; van Esch, J. H. Transient assembly of active materials fueled by a chemical reaction. *Science* **2015**, *349* (6252), 1075-1079.
(8) Maiti, S.; Fortunati, I.; Ferrante, C.; Scrimin, P.; Prins, L. J. Dissipative self-assembly of vesicular nanoreactors. *Nature chemistry* **2016**, *8* (7), 725-731.
(9) Leira-Iglesias, J.; Sorrenti, A.; Sato, A.; Dunne, P. A.; Hermans, T. M. Supramolecular pathway selection of perylenediimides mediated by chemical fuels. *Chemical Communications* **2016**, *52* (58), 9009-9012.
(10) Sharko, A.; Livitz, D.; De Piccoli, S.; Bishop, K. J.; Hermans, T. M. Insights into Chemically Fueled Supramolecular Polymers. *Chemical Reviews* **2022**.
(11) van Rossum, S. A.; Tena-Solsona, M.; van Esch, J. H.; Eelkema, R.; Boekhoven, J. Dissipative out-of-equilibrium assembly of man-made supramolecular materials. *Chemical Society Reviews* **2017**, *46* (18), 5519-5535.
(12) Tena-Solsona, M.; Boekhoven, J. Dissipative self-assembly of peptides. *Israel Journal of Chemistry* **2019**, *59* (10), 898-905.
(13) Klajn, R.; Wesson, P. J.; Bishop, K. J.; Grzybowski, B. A. Writing self-erasing images using metastable nanoparticle "inks". *Angewandte Chemie International Edition* **2009**, *48* (38), 7035-7039.
(14) de Jong, J. J.; Hania, P. R.; Pugžlys, A.; Lucas, L. N.; de Loos, M.; Kellogg, R. M.; Feringa, B. L.; Duppen, K.; van Esch, J. H. Light-driven dynamic pattern formation. *Angewandte Chemie* **2005**, *117* (16), 2425-2428.
(15) Rakotondradany, F.; Whitehead, M.; Lebuis, A. M.; Sleiman, H. F. Photoresponsive supramolecular systems: self-assembly of azodibenzoic acid linear tapes and cyclic tetramers. *Chemistry–A European Journal* **2003**, *9* (19), 4771-4780.
(16) Selmani, S.; Schwartz, E.; Mulvey, J. T.; Wei, H.; Grosvirt-Dramen, A.; Gibson, W.; Hochbaum, A. I.; Patterson, J. P.; Ragan, R.; Guan, Z. Electrically Fueled Active Supramolecular Materials. *Journal of the American Chemical Society* **2022**, *144* (17), 7844-7851.
(17) Angulo-Pachón, C. A.; Miravet, J. F. Sucrose-fueled, energy dissipative, transient formation of molecular hydrogels mediated by yeast activity. *Chemical Communications* **2016**, *52* (31), 5398-5401.
(18) Jo, H.; Sim, S. Programmable Living Materials Constructed with the Dynamic Covalent Interface between Synthetic Polymers and Engineered B. subtilis. *ACS Applied Materials & Interfaces* **2022**, *14* (18), 20729-20738. DOI: 10.1021/acsami.2c03111.
(19) Otto, M. Staphylococcus epidermidis—the'accidental'pathogen. *Nature reviews microbiology* **2009**, *7* (8), 555-567.
(20) Brooks, W. L.; Deng, C. C.; Sumerlin, B. S. Structure–reactivity relationships in boronic acid–diol complexation. *ACS omega* **2018**, *3* (12), 17863-17870.
(21) Lindgren, J.; Thomas, V. C.; Olson, M.; Chaudhari, S.; Nuxoll, A. S.; Schaeffer, C.; Lindgren, K.; Jones, J.; Zimmerman, M. C.; Dunman, P. Arginine deiminase in Staphylococcus epidermidis functions to augment biofilm maturation through pH homeostasis. *Journal of bacteriology* **2014**, *196* (12), 2277-2289.
(22) Marco-Dufort, B.; Iten, R.; Tibbitt, M. W. Linking molecular behavior to macroscopic properties in ideal dynamic covalent networks. *Journal of the American Chemical Society* **2020**, *142* (36), 15371-15385.
(23) Piest, M.; Zhang, X.; Trinidad, J.; Engbersen, J. F. pH-responsive, dynamically restructuring hydrogels formed by reversible crosslinking of PVA with phenylboronic acid functionalised PPO–PEO–PPO spacers (Jeffamines®). *Soft Matter* **2011**, *7* (23), 11111-11118.
(24) Jiang, M.; Li, Q.; Hu, S.; He, P.; Chen, Y.; Cai, D.; Wu, Y.; Chen, S. Enhanced aerobic denitrification performance with Bacillus licheniformis via secreting lipopeptide biosurfactant lichenysin. *Chemical Engineering Journal* **2022**, *434*, 134686.
(25) Allan, D.; Caswell, T.; Keim, N.; van der Wel, C. M.; Verweij, R. soft-matter/trackpy: Trackpy v0. 5.0. *Genève: Zenodo* **2021**.

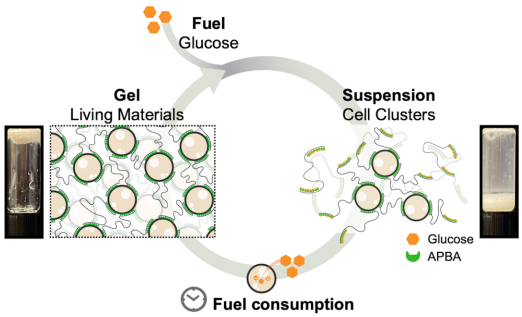
Fuel
Glucose
Gel
Living Materials
Suspension
Cell Clusters
Glucose
APBA
Fuel consumption